Pro-angiogenic activity of salvianolate and its potential therapeutic effect against acute cerebral ischemia

JIAZHEN XU[1,2*], YUE SHEN[3*], PENGWEI LUAN[1*], HAIYING WANG[3], YULAN XU[1], LIXIAN JIANG[1], RUIXIANG LI[1], FEIYUN WANG[1], YUYING ZHU[1] and JIANGE ZHANG[1,4]

[1]Research Center of Chiral Drugs, Innovation Research Institute of Traditional Chinese Medicine, Shanghai University of Traditional Chinese Medicine, Shanghai 201203; [2]Cancer Institute, The Affiliated Hospital of Qingdao University, Qingdao University, Qingdao Cancer Institute, Qingdao, Shandong 266071; [3]School of Pharmacy, Shanghai University of Traditional Chinese Medicine; [4]Shanghai Frontiers Science Center for Traditional Chinese Medicine Chemical Biology, Innovation Research Institute of Traditional Chinese Medicine, Shanghai University of Traditional Chinese Medicine, Shanghai 201203, P.R. China

Received January 30, 2023; Accepted June 23, 2023

DOI: 10.3892/etm.2023.12108

Abstract. Salvianolate (Sal) is a medicinal composition that is widely used in China for the treatment of coronary heart disease and angina pectoris. The aim of the present study was to investigate the potential macrophage-mediated pro-angiogenic effects of Sal *in vitro*. In addition, another aim was to explore the effects of Sal in a rat model of transient middle cerebral artery occlusion (tMCAO) along with the potential mechanism by which it promotes angiogenesis. In this study, human umbilical vein endothelial cells (HUVECs) and Raw264.7 macrophages *in vitro*, and a rat tMCAO model *in vivo* were used to detect the pro-angiogenic effect and mechanism of Sal. The results of *in vitro* experiments showed that the viability, migration and tube formation of HUVECs were promoted by the supernatant of Sal-treated Raw264.7 macrophages (s-Sal) but not by Sal alone. s-Sal also increased the levels of phosphorylated (p-)VEGFR-2, p-AKT and p-p38 MAPK in HUVECs while Sal alone did not. *In vivo*, treatment with Sal significantly reduced the cerebral infarction volume and neurological deficit scores in the rat tMCAO model. Similar to the mechanism observed in the *in vitro* experiments, Sal treatment upregulated the protein expression of VEGF and VEGFR-2, in addition to the phosphorylation of VEGFR-2, AKT and p38, in the brain tissues of the tMCAO model rats. In summary, the results of the present study suggest that the mechanism of Sal-mediated angiogenesis is associated with stimulation of the VEGF/VEGFR-2 signaling pathway by macrophages. This suggests the potential of Sal as a therapeutic option for the treatment of acute cerebral ischemic injury, which may act via the promotion of angiogenesis.

Correspondence to: Dr Yuying Zhu or Professor Jiange Zhang, Research Center of Chiral Drugs, Innovation Research Institute of Traditional Chinese Medicine, Shanghai University of Traditional Chinese Medicine, 1200 Cailun Road, Shanghai 201203, P.R. China
E-mail: ying.yu.zhu@163.com
E-mail: jgzhang@shutcm.edu.cn

*Contributed equally

Key words: salvianolate, ischemic stroke, angiogenesis, macro

Introduction

Stroke is a leading cause of long-term disability among adults and is the third most frequent cause of mortality worldwide. However, no effective treatments are currently available for facilitating recovery from stroke (1,2). Ischemic stroke, which constitutes 80% of all stroke cases, is the most common type of stroke and results from focal cerebral ischemia caused by the occlusion of major cerebral arteries (3). Ischemic stroke is a serious neurological condition that occurs via a complex and varied pathophysiological process, the fine pathophysiological mechanism of which remains to be fully elucidated (4-6). Therefore, it is necessary to devise a novel, safe and effective method that can be used for early stroke treatment as well as for the recovery of motor function lost at the latter stages of stroke.

Angiogenesis, which involves the formation of new blood capillaries from pre-existing blood vessels, serves an important role in the process of tissue remodeling after ischemic stroke (7-9). The reconstruction of new functional microvasculature has been documented to promote recovery from stroke, with angiogenesis being pivotal for repair following ischemic brain injury because it stimulates blood flow and metabolism in the ischemic boundary (10). In addition, angiogenic vessels secrete neurotrophic factors and chemokines, which may create a suitable microenvironment within the damaged brain to support the survival of newly formed neurons (11).

Damage to the brain by cerebral ischemia/reperfusion (I/R) involves multiple reactions, including inflammatory reactions and oxidative damage, and a large number of immune cells, such as macrophages, are typically recruited to the site of

injury (12). These macrophages secrete various angiogenic growth factors, including vascular endothelial growth factor (VEGF), basic fibroblast growth factor and MMP-9 that promote angiogenesis, which can preserve cortical blood supply and improve neurological function during the acute phase of cerebral I/R (13-15). VEGF is an important promoter of post-ischemia neurovascular remodeling (16,17). Ischemia stimulates VEGF expression in the brain (18), thereby promoting the formation of new cerebral blood vessels (19). Furthermore, VEGF has been found to exert mitogenic and anti-apoptotic effects on endothelial cells, which can increase vascular permeability and promote cell migration (20). Among known angiogenic signaling pathways, the VEGF/VEGF receptor-2 (VEGFR2) pathway is especially important, since it can determine when angiogenesis is initiated, the degree of angiogenesis and the type of blood vessels formed. This in turn contributes to the maintenance of normal blood vessel morphology whilst preventing endothelial cell apoptosis. Previous studies have shown that VEGFR2 serves a leading role in the angiogenesis mediated by VEGF (21). Following the binding of VEGF to VEGFR2, autophosphorylation of the receptor occurs, which then activates the downstream MAPK and PI3K/AKT signaling pathways to regulate the migration, survival and proliferation of endothelial cells. This in turn promotes angiogenesis (21).

Salvianolate (Sal) is a medicinal composition derived from the principal active constituents of Danshen. It has been shown to contain magnesium lithospermate B (≥85%), rosmarinic acid (≥10.1%) and lithospermic acid (≥1.9%) (22-24). Danshen is the dried root of the well-known Chinese herb *Salvia miltiorrhiza* Bunge (Labiatae). Due to its ability to promote blood circulation, it is widely used for the treatment of various cardiovascular diseases, including coronary heart disease and angina pectoris, in China (25-27).

In the present study, the potential effects of Sal on endothelial cell and macrophage function and intracellular signaling were investigated *in vitro*. Furthermore, the rat transient middle cerebral artery occlusion (tMCAO) model was used to evaluate the effects of Sal on acute cerebral ischemia *in vivo*.

Materials and methods

Reagents and antibodies. Sal (batch no. 17111321) was obtained from Shanghai Green Valley Pharmaceutical Co., Ltd. DMEM was purchased from Gibco (Thermo Fisher Scientific, Inc.). FBS was purchased from Serana Europe GmbH. VEGF protein (cat. no. 100-20) was purchased from PeproTech, Inc. The rabbit monoclonal antibody against phosphorylated (p)-VEGFR2 (cat. no. 3770), rabbit monoclonal antibody against VEGFR2 (cat. no. 9698), mouse monoclonal antibody against β-actin (cat. no. 3700), rabbit monoclonal antibody against p-AKT (cat. no. 4060), rabbit monoclonal antibody against AKT (cat. no. 4696), rabbit anti-p38 MAPK monoclonal antibody (cat. no. 8690) and rabbit anti-p-p38 monoclonal antibody (cat. no. 4511) were purchased from Cell Signaling Technology, Inc. The mouse anti-F4/80 (C-7) monoclonal antibody (sc-377009) and rabbit anti-VEGF polyclonal antibody (sc-7269) were purchased from Santa Cruz Biotechnology, Inc. The rabbit anti-CD31 polyclonal antibody (GB12063) was purchased from Wuhan Servicebio Technology Co., Ltd. Horseradish peroxidase (HRP)-conjugated goat anti-mouse (A0216) and goat anti-rabbit (A0208) secondary antibodies were purchased from Beyotime Institute of Biotechnology.

Animals. All animal protocols and procedures were approved by the Shanghai University of Traditional Chinese Medicine Institutional Animal Care and Use Committee (grant no. PZSHUTCM200320004). All experiments were performed in accordance with the guidelines described in the Regulations for the Administration of Affairs Concerning Experimental Animals of China enacted in 1988. A total of 97 healthy male Sprague-Dawley rats (8 weeks old; weight, 300±20 g) were purchased from Shanghai Sino-British SIPPR/BK Lab Animal Co., Ltd. The rats were individually caged in a climate-controlled room (20-26˚C, relative humidity of 40-70%) housed under a 12-h dark/light cycle, and allowed free access to water and food. The animals were fasted without water deprivation for 12 h before the tMCAO procedure was performed.

Cell culture. Human umbilical vein endothelial cells (HUVECs; American Type Culture Collection HUV-EC-C cell line, cat. no. CRL-1730) were obtained from the Cancer Research Institute of Central South University. The murine RAW264.7 cell line was purchased from the Institute of Biochemistry and Cell Biology, Chinese Academy of Sciences. Both types of cells were cultured in DMEM containing 10% FBS at 37˚C in a humidified atmosphere comprising 5% CO_2 in an incubator.

Preparation of the RAW264.7 cell supernatant. RAW264.7 cells (~$3x10^6$ cells/ml) were seeded into cell culture dishes (60x15 mm) and incubated for 24 h. The cells were then incubated in medium without or with Sal (10 μM) at 37˚C. After culturing for 24 h, the medium was collected and centrifuged (3,500 x g) to remove cell debris. The following solutions were then collected: i) s-control, comprising the supernatant of RAW264.7 cells; and ii) s-Sal, comprising the supernatant of Sal (10 μM)-treated RAW264.7 cells.

Cell treatment and groups. In total, the following five groups were designated for the treatment of HUVECs: i) Control group, untreated HUVECs; ii) s-control group, where the HUVECs were treated with supernatant of RAW264.7 cells; iii) Sal group, where the HUVECs were treated with 10 μM Sal; iv) s-Sal group, where the HUVECs were treated with supernatant of Sal (10 μM)-treated RAW264.7 cells; and v) VEGF group, where the HUVECs were treated with 10 ng/ml VEGF as a positive control.

Cell viability assay. Cell viability was evaluated using the MTT assay (Sigma-Aldrich; Merck KGaA). HUVECs ($2.5x10^3$ cells/well) were seeded into 96-well culture plates and incubated for 24 h. Subsequently, 100 μl complete medium containing Sal (10 μM), s-control or s-Sal was added. VEGF (10 ng/ml) was added as the positive control. After culturing for 24 h, 20 μl MTT (5 mg/ml) was then added to each well for an additional 4 h, prior to the addition of 150 μl DMSO to dissolve the formazan. The absorbance (optical density value) at 490 nm was detected.

Wounding healing assay. HUVECs ($5x10^5$ cells/well) were seeded into six-well culture plates to form a 90% confluent cell monolayer. The monolayer was scratched vertically along the center of each well with a 200-μl pipette tip and rinsed carefully with PBS three times to remove the cell debris. The HUVECs were incubated for 24 h with Sal (10 μM), s-control, s-Sal or VEGF (10 ng/ml; positive control) in the absence of FBS. In total, three randomly selected views along the wound line in each well were photographed using an inverted light microscope after incubation for 0 and 24 h. ImageJ software 1.50i (National Institutes of Health) was used to analyze the image migration distance and calculate the migration rate (MR). The MR was calculated according to the formula below: MR (%)=(1-24 h scratch distance/0 h scratch distance) x100.

Tube formation assay. A 50-μl volume of Matrigel (BD Biosciences) was pipetted into each well of a pre-chilled 96-well plate and allowed to solidify at 37˚C for 30 min. Subsequently, HUVECs ($5x10^4$ cells/well) and 100 μl culture medium without or with Sal (10 μM), s-control, s-Sal or VEGF (10 ng/ml) were placed into each well and incubated for another 3 h. Tube formation was then observed and photographic images were captured using a Nikon light microscope (Nikon Corporation) and tube formation ability was measured by determining the number of master junctions with ImageJ software 1.50i (National Institutes of Health).

Cell cycle. Cell cycle was detected using flow cytometry. HUVECs ($3x10^5$ per well) were cultured in 60-mm culture plates for 24 h and then incubated with either medium alone or medium containing Sal (10 μM), s-control, s-Sal or VEGF (10 ng/ml) at 37˚C for 24 h. The cell cycle analysis was performed using a Cell Cycle Assay Kit-PI/RNase Staining (cat. no. C543) according to the manufacturer's protocol (Dojindo Molecular Technologies, Inc.). The cell cycle was detected via flow cytometry (CytoFLEX; Beckman coulter, Inc.) and analysis was used ModFit software LT5 (Verity Software House).

Reverse transcription-quantitative PCR (RT-qPCR). RAW264.7 cells ($1x10^6$ per well) were cultured in 60-mm culture plates for 24 h and then incubated without or with varying concentrations of Sal (5, 10, 50, 100 μM) at 37˚C for 3 h. The culture medium was then removed, and total mRNA was extracted from the cells using RNAiso Plus (cat. no. 9108; Takara Bio, Inc.) according to the manufacturer's protocol. Reverse transcription was performed with the PrimeScript™ RT reagent Kit with gDNA Eraser (Perfect Real Time) (cat. no. RR047A; Takara Bio, Inc.), and qPCR was performed using TB Green® Premix Ex Taq™ (Tli RNaseH Plus) (cat. no. RR420A; Takara Bio, Inc.) both according to the manufacturer's instructions. The following thermocycling conditions were used for qPCR: Initial denaturation at 95˚C for 30 sec, denaturation (40 cycles) at 95˚C for 5 sec, and annealing/extending (40 cycles) at 60˚C for 30 sec; melt curve at 95˚C for 15 sec, at 60˚C for 1 min and at 95˚C for 15 sec. β-actin was used as a reference in the experiment. Relative mRNA expression was normalized to β-actin levels and analyzed with the $2^{-\Delta\Delta Cq}$ method (28). The mouse source primers were as follows: β-actin, forward: 5'-GTCCCTCACCCTCCCAAAAG-3' and reverse: 5'-GCTGCCTCAACACCTCAACCC-3'. *Vegf*, forward: 5'-TAGAGTACATCTTCAAGCCGTC-3', reverse: 5'-CTTTCTTTGGTCTGCATTCACA-3'. β-actin was used as the reference gene.

ELISA. RAW264.7 cells ($2x10^6$ per well) were cultured in 60-mm culture plates for 24 h and then incubated without or with 10 μM Sal at 37˚C for 24 h. The medium was collected and centrifuged at 3,500 x g at room temperature for 3 min to remove cell debris. The content of VEGF in the medium was determined using a Mouse VEGF ELISA Kit (cat. no. EMC103.96; Neobioscience Technology Co., Ltd.) according to the manufacturer's protocol.

Western blotting. Brain tissue and cell lysates were prepared using NP40 lysis buffer (Beyotime Institute of Biotechnology). Protein concentrations were determined using the Enhanced BCA Protein Kit (Beyotime Institute of Biotechnology). An equal amount of each sample (30 μg) was separated by 10% SDS-PAGE and then transferred onto PVDF membranes. After blocking with 5% non-fat milk for 2 h at room temperature, the membranes were washed with TBS-10% Tween 20 three times for 10 min each and then incubated with VEGF (1:1,000 dilution), VEGFR-2 (1:1,000 dilution), p-VEGFR-2 (1:1,000 dilution), AKT (1:1,000 dilution), p-AKT (1:1,000 dilution), p38 (1:1,000 dilution) or p-p38 (1:1,000 dilution) antibodies at 4˚C overnight. The membranes were then washed and incubated with the appropriate HRP-conjugated secondary antibody for 1 h at room temperature. The proteins were subsequently detected using a Clarity™ Western ECL Substrate kit (Bio-Rad Laboratories, Inc.). The densitometry analysis used AzureSpot software 2.0.062 (Azure Biosystems, Inc.).

Construction of the rat model of tMCAO. The tMCAO rat model was established using a modified suture occlusion method. Rats were anesthetized with isoflurane (3% for induction and 2.5% for maintenance) before an incision was made in the neck of the rats precisely at the median position. The left common carotid artery (CCA), external carotid artery (ECA) and internal carotid artery (ICA) were carefully isolated. The CCA and ECA were then ligated, before a microaneurysm clip was placed around the ICA. A hole was cut in the CCA and the blunted tip of a nylon suture was inserted through the hole into the ICA until mild resistance was felt. The suture was left in place for 2 h and then withdrawn to allow reperfusion. In the sham-operated group, the rats were anesthetized, but only CCA and ECA ligation was performed.

Neurological functions were evaluated with the Longa scale (29) on the third day after MCAO/reperfusion. The neurological deficits were assessed using the following five-point scale: i) 0 points, no deficit; ii) 1 point, forelimb weakness, flexion of and inability to straighten the contralateral forelimb; iii) 2 points, circling to the affected side; iv) 3 points, inability to bear weight on the affected side and tilting to the contralateral side while walking; and v) 4 points, no spontaneous locomotor activity or loss of consciousness. Animals with scores of 0 or 4 points were excluded from the study.

Treatment and groups. Rats were randomly assigned into the following groups: i) Sham group (n=13), in which sham-operated rats were injected with normal saline by intraperitoneal

injection; ii) infarct group (n=28), in which tMCAO model rats were injected with normal saline 2 h after reperfusion; iii) Sal groups, in which tMCAO rats were intraperitoneally injected with 5 (n=5), 10 (n=5), 20 (n=28) or 40 mg/kg (n=5) Sal 2 h after reperfusion; and iv) ED group (n=13), in which tMCAO model rats were treated with 30 mg/kg edaravone (Zhejiang Shengtong Biotechnology Co., Ltd.) 2 h after reperfusion as a positive control. The treatment was administered for 3 days with a frequency of once a day. To observe the effects of Sal (20 mg/kg) at different time periods, brain tissues were collected after 0, 1 and 3 days from mice in the infarct and Sal groups.

2,3,5-Triphenyltetrazolium chloride (TTC) staining. Rats from the different groups were anesthetized with 2% sodium pentobarbital (30 mg/kg) and then the brain tissues were rapidly collected and cut into 2-mm slices. The brain slices were immersed in 2% TTC (Sigma-Aldrich; Merck KGaA) solution at 37˚C for 15 min, after which they were soaked and fixed in 4% paraformaldehyde solution at room temperature for 15 min. The ischemic area of each brain slice was photographed and analyzed using ImageJ software 1.50i. The infarct area is the area of viable brain tissue in the right hemisphere minus the area of viable brain tissue in the left hemisphere. The infarct volume was calculated according to the following formula:

$$V = \sum_{1}^{n} \left[\left(S_n + \sqrt{S_n \times S_{n+1}} + S_{n+1} \right) \times \frac{h}{3} \right]$$

where h=2 mm, which represents the distance between each section and S represents the infarct area (mm^2) in each brain section.

Histology and H&E staining. At the end of the experiment, the rats were anesthetized with 2% sodium pentobarbital (30 mg/kg) and transcardially perfused with 150 ml PBS. The brain tissues were isolated and fixed in 4% paraformaldehyde solution at 4˚C overnight. The cerebral hemispheres were then cut in the coronal plane, stained with H&E at room temperature for 12 min and examined by light microscopy.

Immunohistochemical staining. Immunohistochemical analysis was performed to detect the expression of VEGF and VEGFR-2. After 3 days, rats were sacrificed by deep anesthesia with 2% sodium pentobarbital (30 mg/kg) followed by transcardial perfusion with PBS, before the brain tissues were fixed with 4% paraformaldehyde at room temperature for 24 h. The 5-μm paraffinized brain sections were dewaxed and dehydrated in xylene and ethanol solutions, followed by antigen retrieval. Briefly, to deparaffinize and rehydrate, the sections were incubated in 3 changes of xylene for 10 min each and then dehydrate in 2 changes of pure ethanol for 5 min, followed by dehydration in gradient ethanol (85 and 75% ethanol) for 5 min each. The sections were then washed in distilled water. For antigen retrieval, the slides were immersed in EDTA antigen retrieval buffer (Wuhan Servicebio Technology Co., Ltd.) and maintained in boiling water for 35 min before being air cooled. The slides were then washed three times with PBS

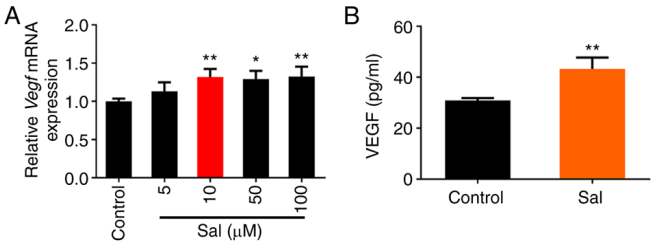

Figure 1. Effect of Sal on the expression of VEGF mRNA and protein in macrophages. (A) Relative *Vegf* mRNA expression levels in RAW264.7 cells. (B) Levels of VEGF protein in the RAW264.7 cell supernatant. Values are presented as the mean ± SD (n=5). *P<0.05, **P<0.01 vs. the control group. Sal, salvianolate; VEGF, vascular endothelial growth factor.

(pH 7.4) in a rocker device, for 5 min each, and blocked with 10% goat serum (Beyotime Institute of Biotechnology) at room temperature for 15 min. All sections were then incubated with anti-VEGF (1:100 dilution) and anti-VEGFR-2 (1:100 dilution) antibodies at 4˚C overnight. The sections were then washed in PBS three times prior to incubation with HRP-conjugated goat anti-rabbit IgG secondary antibodies for 10 min at room temperature. Next, the sections were visualized using a DAB kit and counterstained with hematoxylin at room temperature for 3 min. Using a light microscope, an investigator (FYW) blinded to the experimental groups randomly selected three separate tissue sections for each rat. The staining was analyzed using ImageJ analysis software 1.50i.

Immunofluorescence staining. Paraffin-embedded brain sections were cut to a thickness of 5 μm in the coronal plane, deparaffinized using xylene, rehydrated with a descending ethanol gradient and washed in distilled water, prior to blocking with 10% goat serum (Beyotime Institute of Biotechnology) at room temperature for 1 h. The sections were then incubated with the primary antibodies targeting the following proteins overnight at 4˚C: VEGF (1:100 dilution) and F4/80 (a marker of macrophage cells; 1:350 dilution), or VEGFR-2 (1:100 dilution) and CD31 (a marker of vascular endothelial cells; 1:200 dilution). The sections were then washed in PBS and incubated with the appropriate secondary antibodies, namely anti-mouse IgG Alexa Fluor® 488 Conjugate (cat. no. 4408; Cell Signaling Technology, Inc.) and Cy™3-conjugated Affinipure Donkey anti-rabbit IgG (cat no. 152679; Jackson ImmunoResearch Laboratories, Inc.) for 2 h at room temperature in the dark. The sections were finally mounted on coverslips with a drop of DAPI solution (Sigma-Aldrich; Merck KGaA). The stained cells were observed using a confocal microscope (A1; Nikon Corporation). The staining was analyzed using ImageJ analysis software 1.50i.

Statistical analysis. The neurological score data are presented as the median and interquartile range and were analyzed using the Kruskal-Wallis test followed by Dunn's post-hoc tests. All other data obtained are presented as the mean ± SD and were analyzed statistically using one-way or two-way analysis of variance followed by Bonferroni's multiple-comparisons tests. Statistical analysis was performed using GraphPad 8.0 software (GraphPad Software; Dotmatics). P<0.05 was considered to indicate a statistically significant difference.

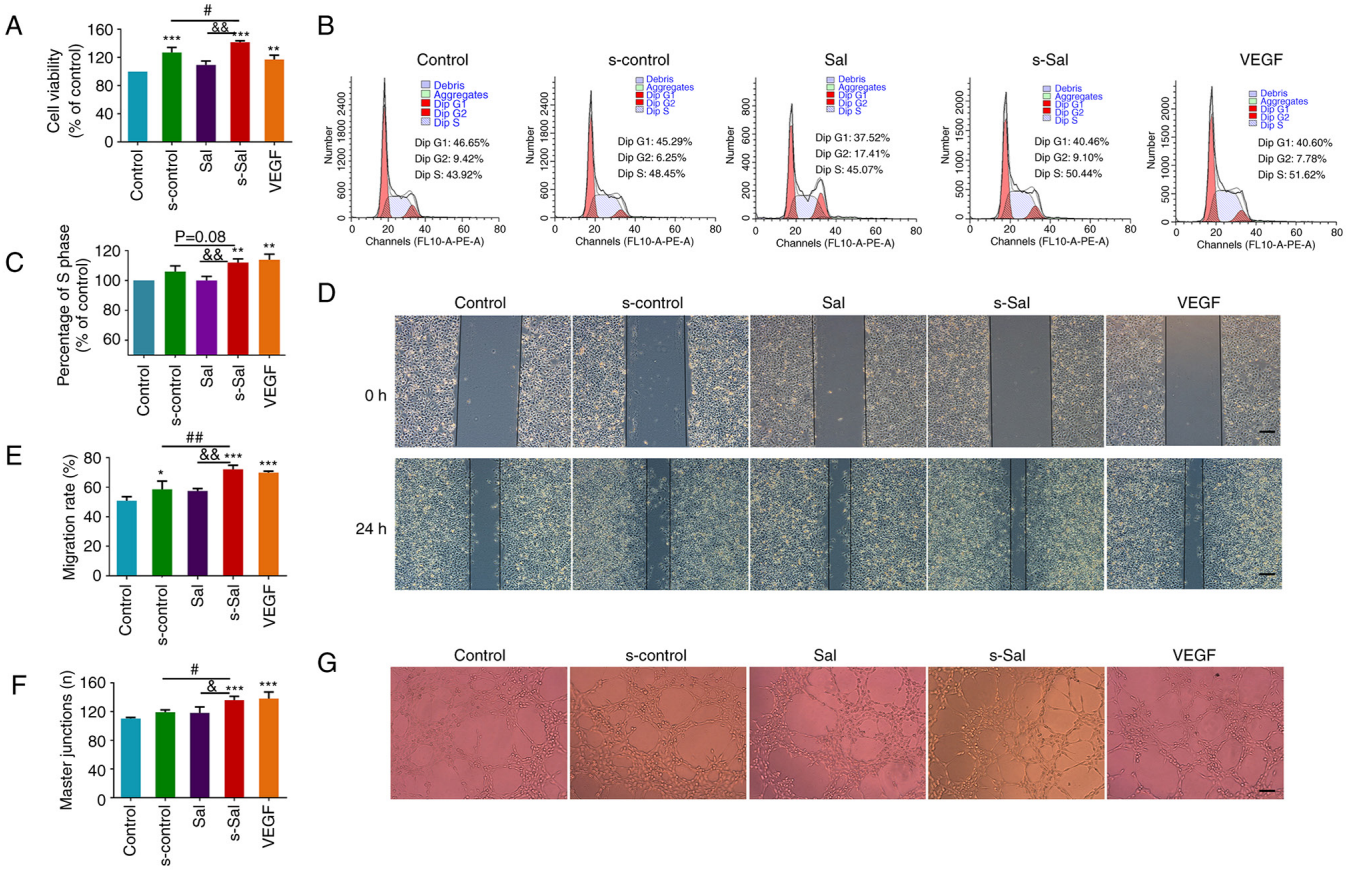

Figure 2. Effect of Sal on the viability, cell cycle, migration and tube formation of HUVECs. (A) Effect of Sal on HUVEC viability. (B) Cell cycle distribution of the HUVECs was detected by flow cytometry and (C) the proportion of cells in the S phase was quantified. (D) Representative images from a wound healing assay of HUVECs at 0 and 24 h (scale bar, 200 μm) and (E) quantitative analysis of cell migration to the wound. (F) Quantitative analysis of tube formation and (G) representative images of tube formation (scale bar, 200 μm). Values are presented as the mean ± SD (n=3 per group); *P<0.05, **P<0.01, ***P<0.001 vs. the control group; $^{\#}$P<0.05, $^{\#\#}$P<0.01, $^{\&}$P<0.05, $^{\&\&}$P<0.01 as indicated. Sal, salvianolate; HUVECs, human umbilical vein endothelial cells; VEGF, vascular endothelial growth factor. Control group, untreated HUVECs; s-control group, HUVECs treated with supernatant of RAW264.7 cells; Sal group, HUVECs treated with 10 μM Sal; s-Sal group, HUVECs treated with supernatant of Sal (10 μM)-treated RAW264.7 cells; VEGF group, HUVECs treated with 10 ng/ml VEGF as a positive control.

Results

Effects of Sal on HUVEC function mediated by macrophages in vitro. Firstly, the effect of Sal on VEGF expression and production in macrophages at the mRNA and protein levels, respectively, was assessed. The results showed that treatment with ≥10 μM Sal significantly promoted the expression of *Vegf* mRNA in RAW264.7 cells, and 10 μM Sal increased the secretion of VEGF protein into the supernatant of the cells (Fig. 1). The viability of HUVECs following various treatments was then evaluated using MTT assays. As shown in Fig. 2A, compared with that in the control group, s-control, s-Sal and VEGF treatment all significantly increased the proliferation of HUVECs, whilst treatment with Sal alone did not affect the viability of HUVECs. This suggests that Sal was unable to promote the proliferation of HUVECs directly. However, s-Sal significantly increased the proliferation of HUVECs compared with that in the s-control group, suggesting that Sal indirectly promoted the proliferation of HUVECs through its effect on macrophages. In addition, the cell cycle of the HUVECs was detected by flow cytometry, whereby s-Sal was found to significantly promote the number of HUVECs in the S phase compared with that in the control and Sal groups (Fig. 2B and C).

The migration of HUVECs was next analyzed using a wound healing assay. The s-control, s-Sal and VEGF groups all showed increased degrees of cell migration to the wounded area after 24 h of incubation compared with that in the control group (Fig. 2D and E). In addition, the migration rate in the s-Sal group was significantly higher compared with that in the Sal and s-control groups.

To examine the effect of Sal on the tubule formation of HUVECs, a tube formation assay was performed using Matrigel. Images of canaliculus formation are presented in Fig. 2G, and tube formation is expressed as the number of master junctions in Fig. 2F. No significant difference was detected between the Sal and control groups. However, s-Sal treatments significantly enhanced the extent of tube formation of the HUVECs compared with that in the s-control group. Together, these results suggest that Sal promoted endothelial cell tube formation via its effect on macrophages.

Effect of Sal on VEGF signaling pathways and macrophage activation in vitro. To investigate the effect of Sal on macrophage-mediated angiogenesis and the VEGF signaling pathway *in vitro*, western blotting was performed. Following VEGF binding to VEGFR2, the proliferation and migration of

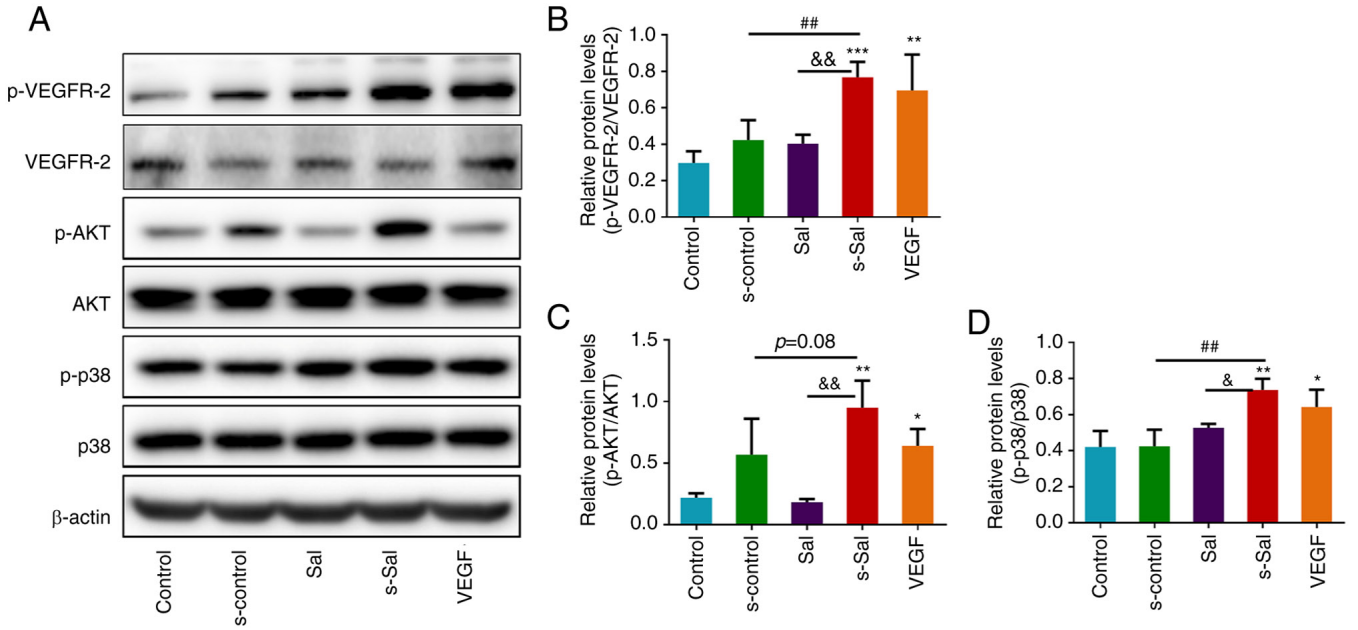

Figure 3. Effect of Sal on the VEGF signaling pathway *in vitro*. (A) Representative western blots of VEGFR-2, p-VEGFR-2, AKT, p-AKT, p38, p-p38 and β-actin. Quantitative analysis of the relative levels of (B) p-VEGFR-2, (C) p-AKT and (D) p-p38 normalized to those of total VEGFR-2, AKT and p38, respectively. Values are presented as the mean ± SD (n=3 per group); *P<0.05, **P<0.01, ***P<0.001 vs. the control group; $^{\#\#}$P<0.01, $^{\&}$P<0.05, $^{\&\&}$P<0.01 as indicated. Sal, salvianolate; VEGF, vascular endothelial growth factor; VEGFR-2, VEGF receptor 2; p-, phosphorylated; Control group, untreated HUVECs; s-control group, HUVECs treated with supernatant of RAW264.7 cells; Sal group, HUVECs treated with 10 μM Sal; s-Sal group, HUVECs treated with supernatant of Sal (10 μM)-treated RAW264.7 cells; VEGF group, HUVECs treated with 10 ng/ml VEGF as a positive control.

endothelial cells and their maturation into vessels are typically activated (7). Therefore, VEGFR2 expression levels and activation were assessed by western blotting analysis (Fig. 3A). s-Sal significantly promoted VEGFR2 phosphorylation at Tyr1175 compared with that in the control, s-control and Sal groups, which indicates that s-Sal induced the activation of this receptor (Fig. 3B). In addition, this form of VEGFR2 activation was found to be associated with the activation of AKT and p38 MAPK signaling downstream (Fig. 3A, C and D), as s-Sal significantly promoted the phosphorylation of AKT compared with that in the control and Sal groups and phosphorylation of p38 proteins compared with that in the control, s-control and Sal groups in the HUVECs. The activation of AKT and p38 MAPK is essential for cellular responses during angiogenesis (7).

Effect of Sal on stroke outcomes. To investigate the possible effects of Sal in the rat tMCAO model, tMCAO model rats were treated with Sal for 3 days and then the neurological deficit scores of the rats were determined. The scores are shown in Fig. 4A. The neurological deficit scores of the infarct group were observed to be significantly increased compared with those in the sham group. A significant reduction in neurological deficit scores of the 10, 20 and 40 mg/kg Sal groups and the ED group was observed compared with that in the infarct group, indicating improved neurological recovery following Sal or ED treatment.

The infarct volume was next determined by TTC staining. The infarct volume was found to be significantly increased in the infarct group compared with the sham group. Rats subjected to cerebral ischemia and treated with various doses of Sal exhibited a significantly smaller infarct volume compared with that in the infarct group (Fig. 4B and C). The neurological deficit scores and infarct volume after treatment with various concentrations of Sal indicated that 20 mg/kg was the most effective concentration, rendering 20 mg/kg as the dose selected for subsequent experiments. The results at the 0-, 1- and 3-day time points for the infarct and 20 mg/kg Sal group indicated that the infarct volume increased and nerve function deteriorated in the infarct group. By contrast, the rats in the Sal-administered group exhibited improvements with reductions in the extent of infarction and nerve function impairment (Fig. 4D-F).

To further investigate the protective effect of Sal against brain I/R injury, morphological changes in the brain tissues were observed by H&E staining after 3 days of treatment with Sal or ED. As shown in Fig. 5A, the characteristic histopathological features in the infarct group were nuclear atrophy, cytoplasmic eosinophilia and cellular edema. The 20 mg/kg Sal treatment group exhibited reduced histopathological abnormalities compared with those in the infarct group.

The effect of Sal on the VEGF signaling pathway was investigated *in vivo*. Immunohistochemical staining (Fig. 5B and C) was used to detect VEGF protein (Fig. 5B and D) and VEGFR-2 protein expression (Fig. 5C and E). The immunohistochemical staining intensity of VEGF and VEGFR-2 in the Sal group was found to be significantly higher compared with that in the infarct group.

Effect of Sal on the VEGF and downstream signaling pathways in vivo. To investigate whether Sal mediates angiogenesis via the VEGF signaling pathway *in vivo*, immunofluorescence analyses were performed. After 3 days of Sal treatment, F4/80 and VEGF double immunofluorescence staining and CD31

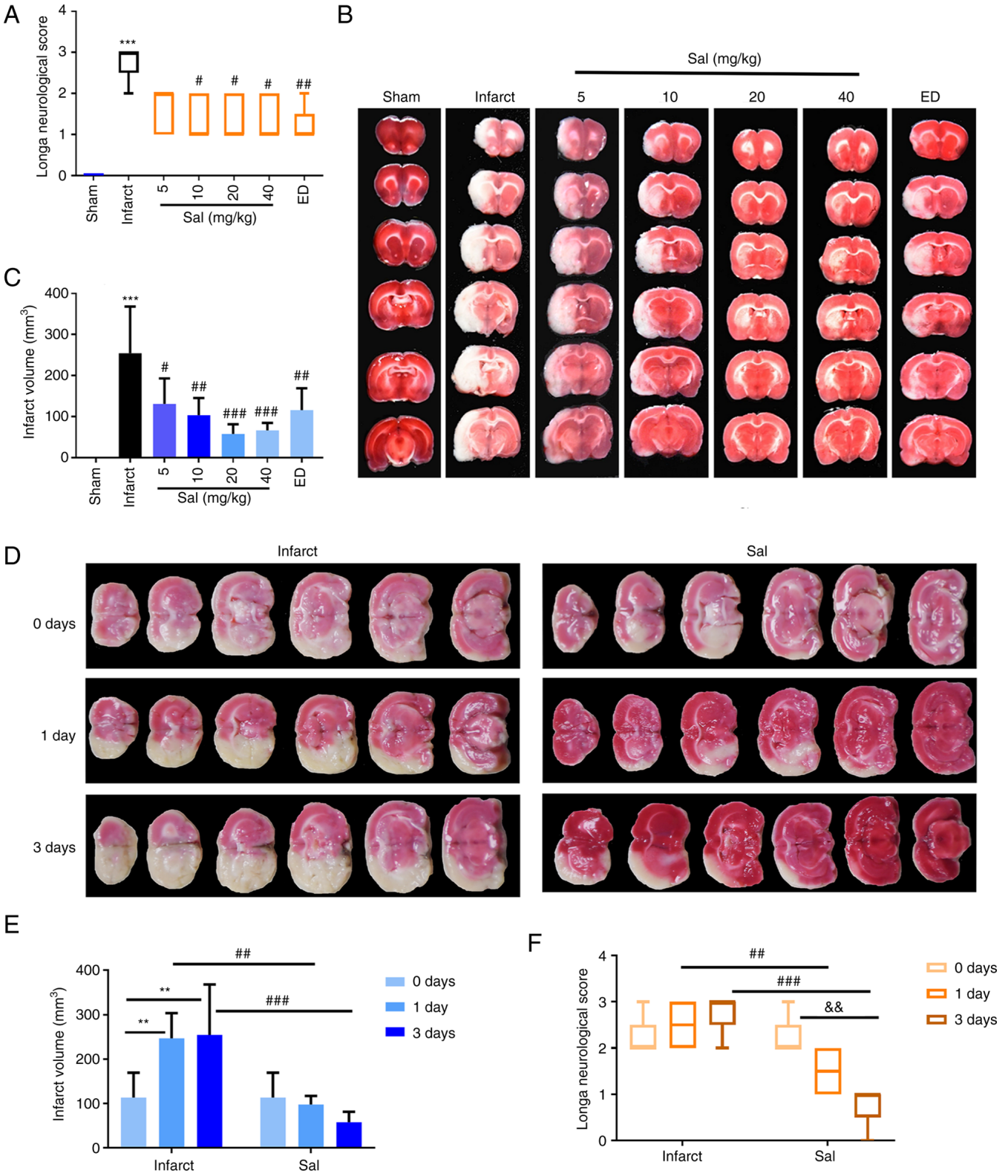

Figure 4. Sal significantly improves stroke outcomes in a rat model of transient middle cerebral artery occlusion. (A) Quantitative analysis of neurological deficit scores. (B) Representative photographs of TTC-stained rat brain slices and (C) quantitative analysis of the cerebral infarct volume following treatment with different concentrations of Sal. ***P<0.001 vs. sham; $^{\#}$P<0.05, $^{\#\#}$P<0.01, $^{\#\#\#}$P<0.001 vs. the infarct group. (D) Representative photographs of TTC-stained rat brain slices and (E) quantitative analysis of the cerebral infarct volume at 0, 1 and 3 days after treatment with or without 20 mg/kg Sal. (F) Quantitative analysis of neurological deficit scores at 0, 1 and 3 days after treatment with or without 20 mg/kg Sal. Values are presented as the median and interquartile range or mean ± SD (n=5 per group). $^{\#\#}$P<0.01, $^{\#\#\#}$P<0.001, **P<0.01, $^{\&\&}$P<0.01 as indicated. Sal, salvianolate; TTC, 2,3,5-triphenyltetrazolium chloride; ED, edaravone.

and VEGFR-2 double immunofluorescence staining were used to detect the cellular location and expression levels of VEGF and VEGFR-2 proteins in the brain tissue (Fig. 6). The results showed that VEGF protein was localized at sites

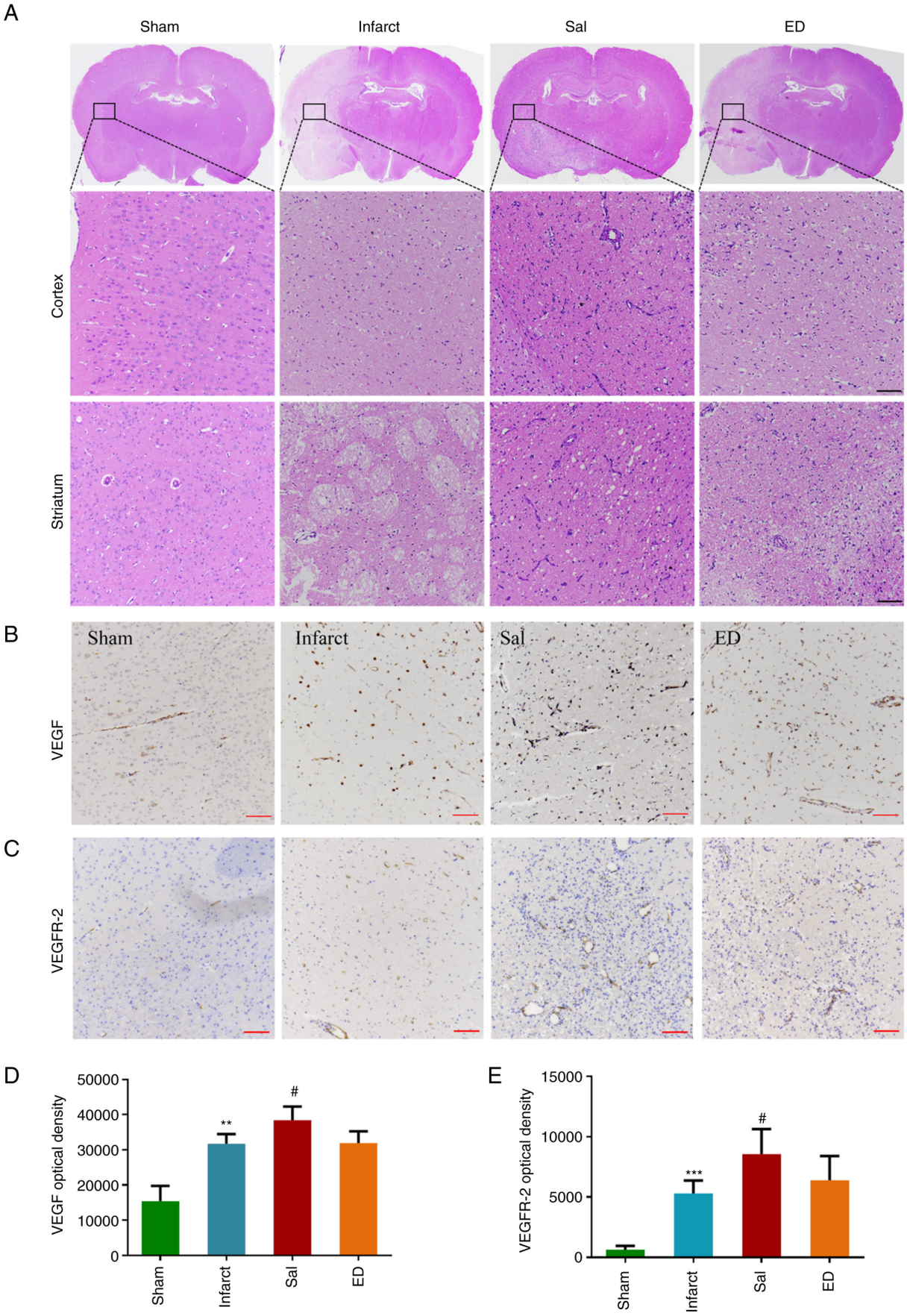

Figure 5. Effect of Sal on the histopathology and protein expression of VEGF and VEGFR-2 in a rat model of transient middle cerebral artery occlusion. (A) H&E-stained cerebral cortex and striatum (scale bar, 100 μm). (B) Representative immunohistochemical images of (B) VEGF and (C) VEGFR-2 staining (scale bar, 100 μm). Quantitative analysis showing the integrated intensity of (D) VEGF and (E) VEGFR-2 staining. Values are presented as the mean ± SD (n=5 per group). **P<0.01, ***P<0.001 vs. the sham group; $^{\#}$P<0.05, vs. the infarct group. Sal, salvianolate; VEGF, vascular endothelial growth factor; VEGFR-2, VEGF receptor 2; ED, edaravone.

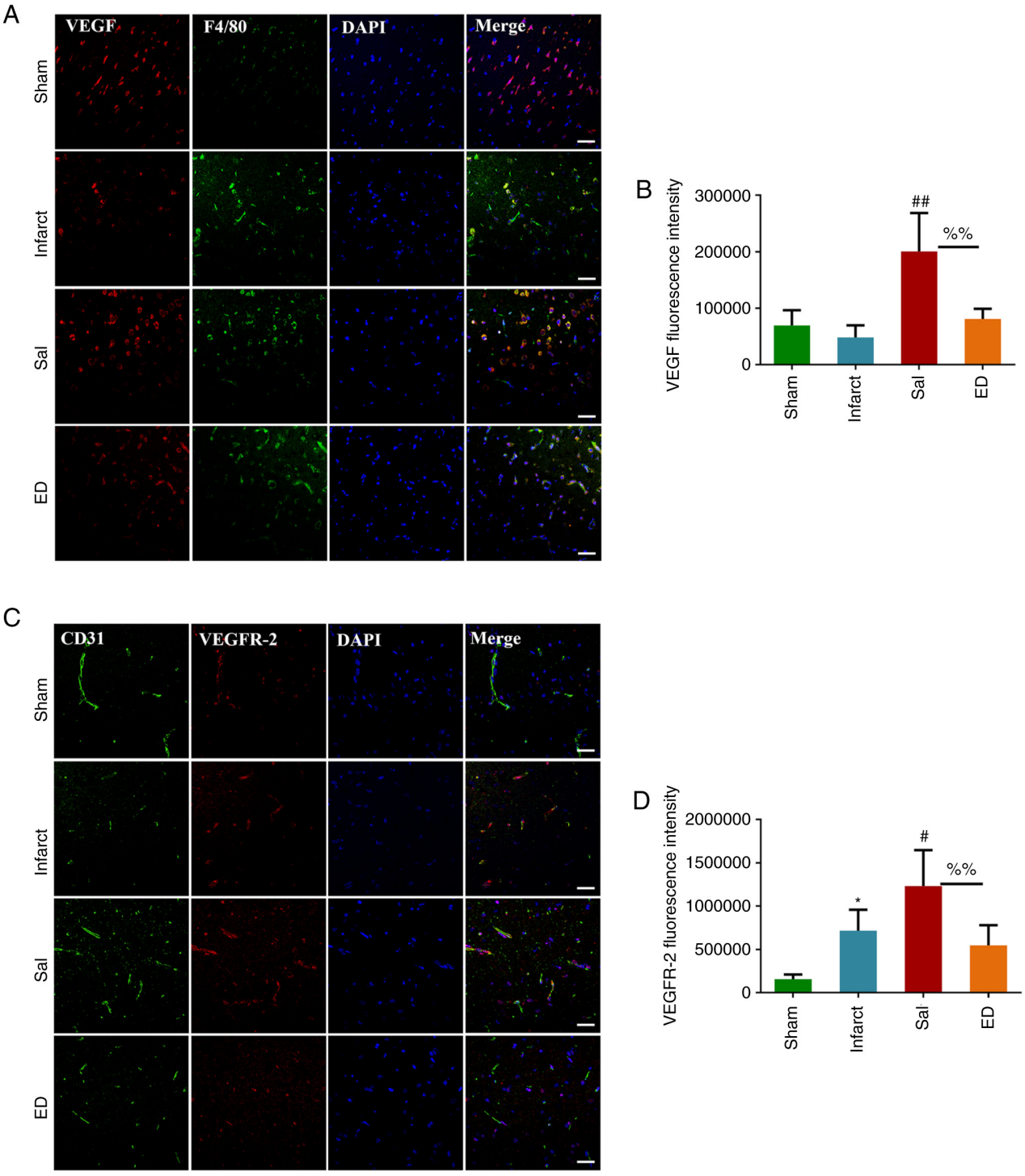

Figure 6. Cellular location and expression of VEGF and VEGFR-2 proteins in the brain tissues of rats with transient middle cerebral artery occlusion. (A) Representative immunofluorescence double staining images of VEGF and F4/80 (scale bar, 100 μm) and (B) the intensity of VEGF immunofluorescence. (C) Representative immunofluorescence double staining images of VEGFR-2 and CD31 (scale bar, 100 μm) and (D) the intensity of VEGFR-2 immunofluorescence. Quantification was performed using ImageJ software. Values are presented as the mean ± SD (n=5 per group). *P<0.05 vs. the sham group; $^{\#}$P<0.05, $^{\#\#}$P<0.01 vs. the infarct group; $^{\%\%}$P<0.01 as indicated. VEGF, vascular endothelial growth factor; VEGFR-2, VEGF receptor 2; Sal, salvianolate; ED, edaravone.

of macrophage accumulation, where it tended to be highly expressed. In addition, VEGFR2 protein was found to colocalize with endothelial cells, and the expression of VEGFR2 in the Sal group was significantly increased compared with that in the infarct group, with higher microvessel density in the former.

To evaluate the efficacy of Sal in upregulating VEGF signaling activity *in vivo*, western blot analysis was performed on tissues in the peri-infarct area. As shown in the western blots in Fig. 7A, VEGF and VEGFR2 protein expression and VEGFR2 phosphorylation in the infarct group were lower compared with those in the sham group. Additionally,

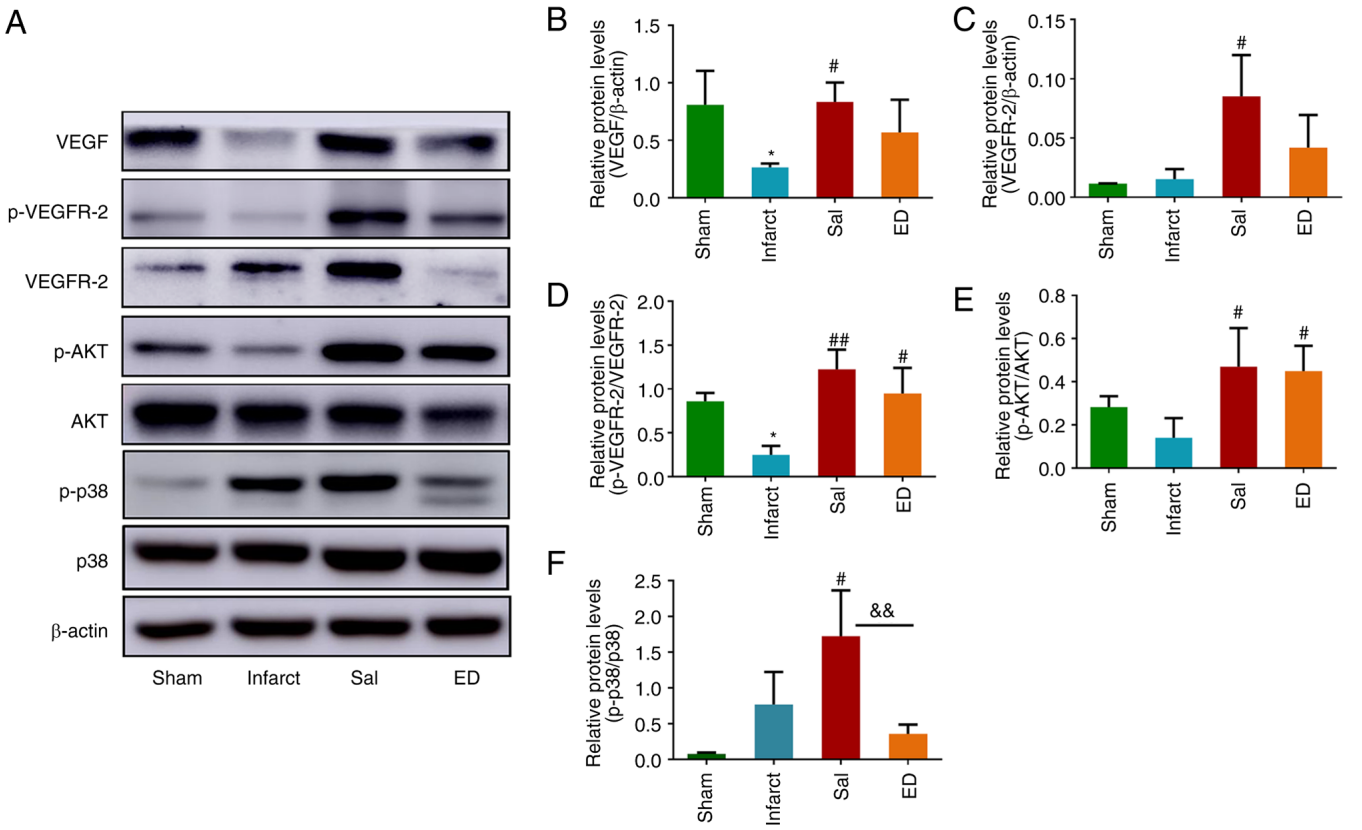

Figure 7. Effect of Sal on the VEGF signaling pathway in a rat model of transient middle cerebral artery occlusion. (A) Representative western blots of VEGF, VEGFR-2, p-VEGFR-2, p-AKT, AKT, p38, p-p38 and β-actin. Quantitative analysis of the relative levels of (B) VEGF and (C) VEGFR-2 normalized to those of β-actin, (D) p-VEGFR-2 relative to those of total VEGFR-2, (E) p-AKT relative to those of total AKT and (F) p-p38 relative to those of total p38. Values are presented as the mean ± SD (n=3 per group). *P<0.05 vs. the sham group; $^{\#}$P<0.05, $^{\#\#}$P<0.01 vs. the infarct group; $^{\&\&}$P<0.01 as indicated. Sal, salvianolate; VEGF, vascular endothelial growth factor; VEGFR-2, VEGF receptor 2; p-, phosphorylated; ED, edaravone.

the protein expression of VEGF (Fig. 7B) and VEGFR2 (Fig. 7C) along with VEGFR-2 phosphorylation (Fig. 7D) were upregulated in the Sal group compared with those in the infarct group. The phosphorylation levels of AKT and p38, which lie downstream of the VEGF/VEGFR2 signaling pathway, were also significantly increased by the administration of Sal (Fig. 7A, E and F). These results suggest that Sal protected rats against acute cerebral ischemia by promoting angiogenesis in the brain. Specifically, the mechanism of its pro-angiogenic activity appears to be the promotion of VEGF signaling and in turn the downstream AKT and p38 signaling pathways.

Discussion

Sal can be extracted from the Chinese herb *Salvia miltiorrhiza* Bunge (Labiatae) and has been widely used for the treatment of cardiovascular diseases, including coronary heart disease and angina pectoris in China. This is due to its reported effect as a promotor of blood circulation. Although the present study demonstrated that Sal exerted no significant effects on HUVECs directly, 10 μM Sal treatment increased *Vegf* mRNA expression in macrophages, which consequently enhanced the secretion of VEGF into the macrophage supernatant. Based on these results, it may be hypothesized that Sal mediated the activation of RAW264.7 macrophages and secretion of VEGF to induce angiogenesis in HUVECs. The pro-angiogenic effects of Sal-treated macrophages, including the promotion of cell proliferation, migration and tube formation were therefore investigated. VEGFR2 is known to regulate vascular endothelial cell proliferation, migration, differentiation and capillary formation (7). Therefore, the promotion of VEGFR2 signaling represents a viable approach for therapeutical pro-angiogenic interventions. In the present study, Sal was found to promote VEGFR2 activation and thereby induce AKT and p38 signaling downstream in HUVECs *in vitro*, via its effect on RAW264.7 cells. Considering that Sal was found to promote angiogenesis via VEGF and downstream signaling pathways *in vitro*, an *in vivo* ischemic stroke model was then established to verify the protective effects of Sal.

Ischemic stroke is a serious neurological disease, the fine pathophysiological mechanism of which remains to be fully elucidated. There are various proposed theories regarding the pathological mechanism underlying I/R injury, which include excitatory amino acids, inflammatory reactions, oxidative stress damage, metabolic acidosis, intracellular Ca^{2+} overload, mitochondrial damage, brain cell apoptosis, necrosis and autophagy (6,30,31). At present, there is no effective long-term treatment method for ischemic stroke. The main treatment measure is early thrombolysis (32). Although thrombolytic treatment can return blood supply to the ischemic area quickly, due to the strict time 3-h window post-ischemia during which the blood supply must be restored and possible

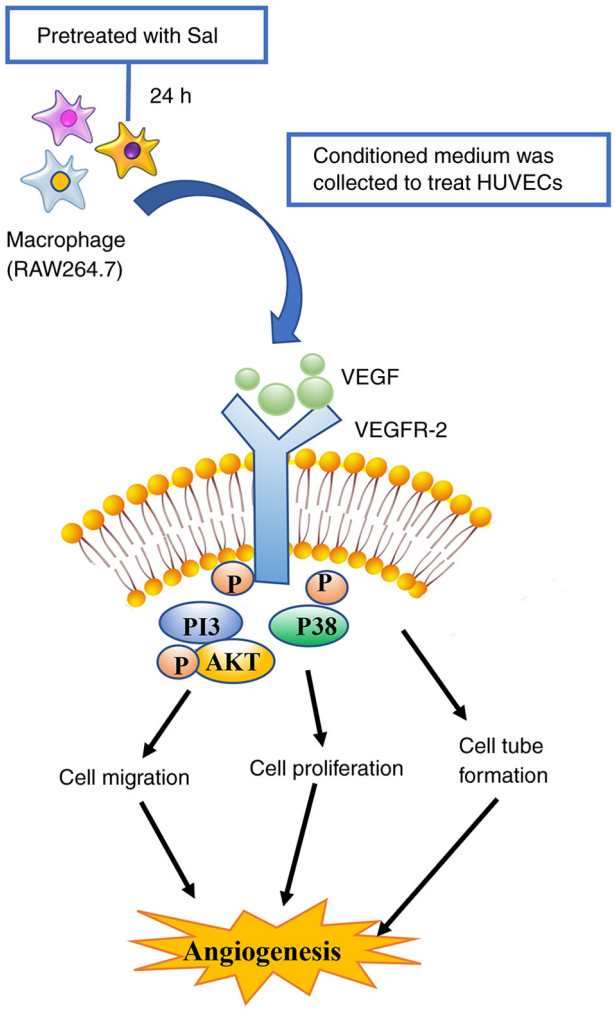

Figure 8. Schematic diagram of the proposed molecular mechanisms underlying the protective effects of Sal treatment against cerebral ischemia-reperfusion injury, which involves macrophage activation-induced HUVEC angiogenesis. Sal, salvianolate; HUVECs, human umbilical vein endothelial cells; VEGF, vascular endothelial growth factor; VEGFR-2, VEGF receptor 2; p, phosphorylated.

adverse reactions, including reperfusion injury and increased hemorrhage risk, its use is limited. Although neurotrophic and neurological rehabilitation are the main treatment objectives, the clinical application of neuroprotective agents has not achieved promising results (33). Therapeutic interventions that involve manipulation of the cellular immune system are currently being explored in patients with ischemic stroke (34,35). Although several studies have previously shown that stem cell therapy can enhance functional recovery from stroke, this treatment is limited by the low survival rate and poor differentiation of transplanted cells (36,37).

The current understanding of immunomodulation in the brain is insufficient, which is largely due to potential drugs not being successful in clinical trials. Therefore, it is necessary to find a safe and effective method that is suitable for use in both early stroke treatment and the recovery of motor functions after stroke. Unfortunately, there is no one therapeutic strategy that can effectively meet the aforementioned conditions. Therefore, further research and development of novel agents is necessary. Ischemic stroke can cause ischemia and hypoxia in the brain tissues, leading to the loss of functional neurons in the corresponding brain areas. The potentially salvageable tissue around the ischemic core, referred to as the penumbra, is the prime region to be targeted (38). The penumbra is unstable with the potential to regenerate, which forms the basis for the treatment of ischemia (1). Previous studies have found that angiogenesis and the rapid establishment of collateral circulation in the area of cerebral infarction and cerebral ischemia can significantly reduce the cerebral infarct size, improve neurobehavioral symptoms and reduce mortality in animals and patients (1,2,39).

For the treatment of ischemic diseases, the promotion of angiogenesis in the ischemic site and its periphery is a promising approach for restorative therapy. In the present study, the administration of Sal to rats following MCAO significantly enhanced neovascularization, restored vascular function and ameliorated neurological deficits. In addition, Sal was found to have beneficial effects on the cortical tissue around the infarct after MCAO. Sal was indicated to attenuate cerebral I/R injury via upregulation of the VEGF/VEGFR2 signaling pathway. According to the *in vivo* results, the expression of the VEGF signaling pathway components VEGF and VEGFR-2 was significantly increased after treatment with Sal. The phosphorylation of VEGFR-2 and its downstream signaling components AKT and p38 were subsequently measured, and the results showed that Sal promoted the phosphorylation of VEGFR-2, AKT and p38. These results support the hypothesis that Sal can regulate endothelial cell function and intracellular signaling through macrophages *in vitro*.

The present study revealed that Sal promoted macrophage-mediated HUVEC proliferation, migration and tube formation. This was associated with the Sal-induced upregulation of VEGFR2, AKT and p38 activation in HUVECs. In addition, Sal accelerated blood vessel formation in a rat model of ischemic stroke whilst upregulating the protein expression of VEGF and VEGFR2, in addition to the activation of VEGFR2, AKT and p38 *in vivo*. This suggests that the mechanism of its pro-angiogenic activity is likely to mainly involve the promotion of VEGF signaling and then AKT and p38 signaling downstream. The protective effect of Sal on rats with acute cerebral ischemia may have been achieved through the promotion of cerebral angiogenesis. These results suggest that Sal is a promising candidate for the treatment of acute cerebral ischemia. The present study has certain limitations and further studies are required to explore improvements. For example, although edaravone has a protective effect against cerebral infarction *in vivo*, its main mechanism of action is to reduce oxidative stress caused by cerebral ischemic injury (40). Drugs associated with angiogenesis will be selected as positive controls in subsequent studies. In addition, the hypothesis that the pro-angiogenic effect of Sal is mediated by blocking the VEGFR-2 signaling pathway will be further verified in the future.

In summary, the results of the present study suggest that Sal regulated endothelial cell function through VEGF and its downstream signaling pathways, likely in a macrophage-dependent manner, *in vitro*. In addition, the protective effect of Sal was verified further in a model of cerebral

ischemia, the mechanism of which is summarized in Fig. 8. These findings shed light on the novel therapeutic effects of the administration of Sal, which may provide information useful for the development of drug leads and candidates for the treatment of ischemic disease.

Acknowledgements

Not applicable.

Funding

This study was supported by grants from the National Natural Science Foundation of China (grant no. 82003800), the Shanghai Municipal Education Commission (grant no. 2019-01-07-00-10-E00072), Shanghai Municipal Health Commission/Shanghai Municipal Administration of Traditional Chinese Medicine [grant no. ZY(2021-2023)-0501], Shanghai Science and Technology Development Fund from Central Leading Local Government (grant no. YDZX20223100001004), Science and Technology Commission of Shanghai Municipality (grant no. 20ZR1473200), 'Chenguang Program' supported by Shanghai Education Development Foundation and Shanghai Municipal Education Commission (grant no. 21CGA51), Open Project of National Major Scientific and Technological Infrastructure for Translational Medicine (Shanghai) (grant no. TMSK-2021-405) and Open Project of Shanghai Key Laboratory for Molecular Engineering of Chiral Drugs (grant no. SMECD2022004).

Availability of data and materials

The datasets used and/or analyzed during the current study are available from the corresponding author on reasonable request.

Authors' contributions

JZ, JX and PL were responsible for study conception and design. JX, YS, YX, LJ, RL and FW performed experiments and analyzed the data. JX and JZ interpreted the data and drafted the manuscript. HW and YZ helped with the data analysis. JZ, YZ, JX and HW edited the manuscript. All authors read and approved the final version of the manuscript. JZ and YZ confirm the authenticity of all the raw data.

Ethics approval and consent to participate

All animal experiments were approved by the Ethics Committee of the animal experiment center of Shanghai University of Traditional Chinese Medicine (Shanghai, China; approval no. PZSHUTCM200320004).

Patient consent for publication

Not applicable.

Competing interests

The authors declare that they have no competing interests.

References

1. Guo H, Adah D, James PB, Liu Q, Li G, Ahmadu P, Chai L, Wang S, Liu Y and Hu L: Xueshuantong injection (lyophilized) attenuates cerebral ischemia/reperfusion injury by the activation of Nrf2-VEGF pathway. Neurochem Res 43: 1096-1103, 2018.
2. Xu H, Cao Y, Yang X, Cai P, Kang L, Zhu X, Luo H, Lu L, Wei L, Bai X, *et al*: ADAMTS13 controls vascular remodeling by modifying VWF reactivity during stroke recovery. Blood 130: 11-22, 2017.
3. Yin KJ, Hamblin M and Chen YE: Angiogenesis-regulating microRNAs and ischemic stroke. Curr Vasc Pharmacol 13: 352-365, 2015.
4. Deb P, Sharma S and Hassan KM: Pathophysiologic mechanisms of acute ischemic stroke: An overview with emphasis on therapeutic significance beyond thrombolysis. Pathophysiology 17: 197-218, 2010.
5. Feng D, Wang B, Wang L, Abraham N, Tao K, Huang L, Shi W, Dong Y and Qu Y: Pre-ischemia melatonin treatment alleviated acute neuronal injury after ischemic stroke by inhibiting endoplasmic reticulum stress-dependent autophagy via PERK and IRE1 signalings. J Pineal Res 62, 2017.
6. Puyal J, Ginet V and Clarke PG: Multiple interacting cell death mechanisms in the mediation of excitotoxicity and ischemic brain damage: A challenge for neuroprotection. Prog Neurobiol 105: 24-48, 2013.
7. Liu Y, Xu J, Zong A, Wang J, Liu Y, Jia W, Jin J, Yan G and Zhang Y: Anti-angiogenic activity and mechanism of a chemically sulfated natural glucan from Phellinus ribis. Int J Biol Macromol 107: 2475-2483, 2018.
8. Thiyagarajan M, Fernández JA, Lane SM, Griffin JH and Zlokovic BV: Activated protein C promotes neovascularization and neurogenesis in postischemic brain via protease-activated receptor 1. J Neurosci 28: 12788-12797, 2008.
9. Zhao BQ, Wang S, Kim HY, Storrie H, Rosen BR, Mooney DJ, Wang X and Lo EH: Role of matrix metalloproteinases in delayed cortical responses after stroke. Nat Med 12: 441-445, 2006.
10. Zhang ZG and Chopp M: Neurorestorative therapies for stroke: underlying mechanisms and translation to the clinic. Lancet Neurol 8: 491-500, 2009.
11. Cattin AL, Burden JJ, Van Emmenis L, Mackenzie FE, Hoving JJ, Garcia Calavia N, Guo Y, McLaughlin M, Rosenberg LH, Quereda V, *et al*: Macrophage-Induced blood vessels guide schwann cell-mediated regeneration of peripheral nerves. Cell 162: 1127-1139, 2015.
12. Manoonkitiwongsa PS, Schultz RL, Whitter EF and Lyden PD: Contraindications of VEGF-based therapeutic angiogenesis: Effects on macrophage density and histology of normal and ischemic brains. Vascul Pharmacol 44: 316-325, 2006.
13. Liu J, Wang Y, Akamatsu Y, Lee CC, Stetler RA, Lawton MT and Yang GY: Vascular remodeling after ischemic stroke: Mechanisms and therapeutic potentials. Prog Neurobiol 115: 138-156, 2014.
14. Pedragosa J, Salas-Perdomo A, Gallizioli M, Cugota R, Miró-Mur F, Briansó F, Justicia C, Pérez-Asensio F, Marquez-Kisinousky L, Urra X, *et al*: CNS-border associated macrophages respond to acute ischemic stroke attracting granulocytes and promoting vascular leakage. Acta Neuropathol Commun 6: 76, 2018.
15. Manoonkitiwongsa PS, Jackson-Friedman C, McMillan PJ, Schultz RL and Lyden PD: Angiogenesis after stroke is correlated with increased numbers of macrophages: The clean-up hypothesis. J Cereb Blood Flow Metab 21: 1223-1231, 2001.
16. Li WL, Fraser JL, Yu SP, Zhu J, Jiang YJ and Wei L: The role of VEGF/VEGFR2 signaling in peripheral stimulation-induced cerebral neurovascular regeneration after ischemic stroke in mice. Exp Brain Res 214: 503-513, 2011.
17. Lee DH, Lee J, Jeon J, Kim KJ, Yun JH, Jeong HS, Lee EH, Koh YJ and Cho CH: Oleanolic acids inhibit vascular endothelial growth factor receptor 2 signaling in endothelial cells: Implication for anti-angiogenic therapy. Mol Cells 41: 771-780, 2018.
18. Wise GE and Yao S: Expression of vascular endothelial growth factor in the dental follicle. Crit Rev Eukaryot Gene Expr 13: 173-180, 2003.
19. Krum JM, Mani N and Rosenstein JM: Angiogenic and astroglial responses to vascular endothelial growth factor administration in adult rat brain. Neuroscience 110: 589-604, 2002.

20. Melincovici CS, Boşca AB, Şuşman S, Mărginean M, Mihu C, Istrate M, Moldovan IM, Roman AL and Mihu CM: Vascular endothelial growth factor (VEGF)-key factor in normal and pathological angiogenesis. Rom J Morphol Embryol 59: 455, 2018.
21. Greenberg DA and Jin K: From angiogenesis to neuropathology. Nature 438: 954-959, 2005.
22. Watzke A, O'Malley SJ, Bergman RG and Ellman JA: Reassignment of the configuration of salvianolic acid B and establishment of its identity with lithospermic acid B. J Nat Prod 69: 1231-1233, 2006.
23. Han B, Zhang X, Zhang Q, Zhao G, Wei J, Ma S, Zhu W and Wei M: Protective effects of salvianolate on microvascular flow in a porcine model of myocardial ischaemia and reperfusion. Arch Cardiovasc Dis 104: 313-324, 2011.
24. Qin CZ, Ren X, Zhou HH, Mao XY and Liu ZQ: Inhibitory effect of salvianolate on human cytochrome P450 3A4 in vitro involving a noncompetitive manner. Int J Clin Exp Med 8: 15549-15555, 2015.
25. Li X, Xu X, Wang J, Wang X, Yang H, Xu H, Tang S, Li Y, Yang L, Huang L, *et al*: A system-level investigation into the mechanisms of Chinese traditional medicine: Compound Danshen formula for cardiovascular disease treatment. PLoS One 7: e43918, 2012.
26. Wu JR, Liu S, Zhang XM and Zhang B: Danshen injection as adjuvant treatment for unstable angina pectoris: A systematic review and meta-analysis. Chin J Integr Med 23: 306-311, 2017.
27. Dong P, Hu H, Guan X, Ung COL, Shi L, Han S and Yu S: Cost-consequence analysis of salvianolate injection for the treatment of coronary heart disease. Chin Med 13: 28, 2018.
28. Zhu Y, Yang L, Xu J, Yang X, Luan P, Cui Q, Zhang P, Wang F, Li R, Ding X, *et al*: Discovery of the anti-angiogenesis effect of eltrombopag in breast cancer through targeting of HuR protein. Acta Pharm Sin B 10: 1414-1425, 2020.
29. Longa EZ, Weinstein PR, Carlson S and Cummins R: Reversible middle cerebral artery occlusion without craniectomy in rats. Stroke 20: 84-91, 1989.
30. Luo Y, Tang H, Li H, Zhao R, Huang Q and Liu J: Recent advances in the development of neuroprotective agents and therapeutic targets in the treatment of cerebral ischemia. Eur J Med Chem 162: 132-146, 2019.
31. Bielewicz J, Kurzepa J, Łagowska-Lenard M and Bartosik-Psujek H: The novel views on the patomechanism of ischemic stroke. Wiad Lek 63: 213-220, 2010 (In Polish).
32. Cohen JE, Leker RR and Rabinstein A: New strategies for endovascular recanalization of acute ischemic stroke. Neurol Clin 31: 705-719, 2013.
33. Weintraub MI: Thrombolysis (tissue plasminogen activator) in stroke: A medicolegal quagmire. Stroke 37: 1917-1922, 2006.
34. Fu Y, Zhang N, Ren L, Yan Y, Sun N, Li YJ, Han W, Xue R, Liu Q, Hao J, *et al*: Impact of an immune modulator fingolimod on acute ischemic stroke. Proc Natl Acad Sci USA 111: 18315-18320, 2014.
35. Fu Y, Liu Q, Anrather J and Shi FD: Immune interventions in stroke. Nat Rev Neurol 11: 524-535, 2015.
36. Carmichael ST: Emergent properties of neural repair: Elemental biology to therapeutic concepts. Ann Neurol 79: 895-906, 2016.
37. Parr AM, Tator CH and Keating A: Bone marrow-derived mesenchymal stromal cells for the repair of central nervous system injury. Bone Marrow Transplant 40: 609-619, 2007.
38. Li D, Lang W, Zhou C, Wu C, Zhang F, Liu Q, Yang S and Hao J: Upregulation of microglial ZEB1 ameliorates brain damage after acute ischemic stroke. Cell Rep 22: 3574-3586, 2018.
39. Hillen F and Griffioen AW: Tumour vascularization: Sprouting angiogenesis and beyond. Cancer Metastasis Rev 26: 489-502, 2007.
40. Yagi K, Kitazato KT, Uno M, Tada Y, Kinouchi T, Shimada K and Nagahiro S: Edaravone, a free radical scavenger, inhibits MMP-9-related brain hemorrhage in rats treated with tissue plasminogen activator. Stroke 40: 626-631, 2009.